Systems/Circuits

Binocular Neuronal Processing of Object Motion in an Arthropod

Florencia Scarano,[1] Julieta Sztarker,[1,2] Violeta Medan,[1,2] Martín Berón de Astrada,[1,2] and Daniel Tomsic[1,2]
[1]Instituto de Fisiología, Biología Molecular y Neurociencias CONICET, Argentina and [2]Departamento de Fisiología, Biología Molecular y Celular Dr. Héctor Maldonado, Universidad de Buenos Aires, Facultad de Ciencias Exactas y Naturales, 1428 Buenos Aires, Argentina

Animals use binocular information to guide many behaviors. In highly visual arthropods, complex binocular computations involved in processing panoramic optic flow generated during self-motion occur in the optic neuropils. However, the extent to which binocular processing of object motion occurs in these neuropils remains unknown. We investigated this in a crab, where the distance between the eyes and the extensive overlapping of their visual fields advocate for the use of binocular processing. By performing *in vivo* intracellular recordings from the lobula (third optic neuropil) of male crabs, we assessed responses of object-motion-sensitive neurons to ipsilateral or contralateral moving objects under binocular and monocular conditions. Most recorded neurons responded to stimuli seen independently with either eye, proving that each lobula receives profuse visual information from both eyes. The contribution of each eye to the binocular response varies among neurons, from those receiving comparable inputs from both eyes to those with mainly ipsilateral or contralateral components, some including contralateral inhibition. Electrophysiological profiles indicated that a similar number of neurons were recorded from their input or their output side. In monocular conditions, the first group showed shorter response delays to ipsilateral than to contralateral stimulation, whereas the second group showed the opposite. These results fit well with neurons conveying centripetal and centrifugal information from and toward the lobula, respectively. Intracellular and massive stainings provided anatomical support for this and for direct connections between the two lobulae, but simultaneous recordings failed to reveal such connections. Simplified model circuits of interocular connections are discussed.

Key words: **behavior; binocularity; giant neurons; *in vivo* intracellular recording; insect vision; optic neuropils**

Significance Statement

Most active animals became equipped with two eyes, which contributes to functions like depth perception, objects spatial location, and motion processing, all used for guiding behaviors. In visually active arthropods, binocular neural processing of the panoramic optic flow generated during self-motion happens already in the optic neuropils. However, whether binocular processing of single-object motion occurs in these neuropils remained unknown. We investigated this in a crab, where motion-sensitive neurons from the lobula can be recorded in the intact animal. Here we demonstrate that different classes of neurons from the lobula compute binocular information. Our results provide new insight into where and how the visual information acquired by the two eyes is first combined in the brain of an arthropod.

Introduction

Highly visual arthropods perform many behaviors by processing panoramic as well as object motion binocularly. In fact, some rely on binocular information of panoramic motion, i.e., the retinal optic flow generated during self-motion, to control their course of navigation (Nalbach et al., 1993; Krapp et al., 2001; Duistermars et al., 2012), whereas others use binocular processing to estimate object size and distance in the context of prey capture behavior (Collet, 1987; Nityananda et al., 2016). To fulfill these functions, information acquired separately by each eye must combine to be computed by binocular neurons in the brain. Binocular neurons responsive either to panoramic optic flow or to object motion have been identified in central areas of the brain of crustaceans and insects (crayfish, *Procambarus clarkii*: Wood and Glantz, 1980a,b; blowfly, *Calliphora vicina*: Wertz et al., 2008; locust, *Schistocerca gregaria*: Rosner and Homberg, 2013). Furthermore, it is well known that binocular computations involved in processing panoramic optic flow already take place in the optic neuropils (e.g., blowfly, *Calliphora vicina*: Krapp et al., 2001;

Received Dec. 27, 2017; revised June 2, 2018; accepted June 5, 2018.

Author contributions: J.S. and D.T. edited the paper; D.T. wrote the first draft of the paper. F.S., J.S., and D.T. designed research; F.S., V.M., and M.B.d.A. performed research; F.S., J.S., V.M., M.B.d.A., and D.T. analyzed data; F.S., J.S., and D.T. wrote the paper.

This work was supported by Grant PICT 2013-0450 from Agencia Nacional de Promoción Científica y Tecnológica and Grant 20020130100583BA (Universidad de Buenos Aires Ciencia y Tecnología) from the University of Buenos Aires to D.T.

The authors declare no competing financial interests.

Correspondence should be addressed to Dr. Daniel Tomsic, Ciudad Universitaria, Pabellón II, Piso 2, FBMC-FCEN, 1428 Buenos Aires, Argentina. E-mail: tomsic@fbmc.fcen.uba.ar.

DOI:10.1523/JNEUROSCI.3641-17.2018

 0270-6474/18/386933-16$15.00/0

Hennig et al., 2011; fly, *Drosophila melanogaster*: Suzuki et al., 2014). Contrasting, the extent to which binocular processing of object motion occurs in the arthropod's optic neuropils remains unknown (but see Dunbier et al., 2012).

The visual system of insects and malacostracan crustaceans are thought to be homologous (Strausfeld, 2009; Sombke and Harzsch, 2015), containing the retina and a series of retinotopic neuropils that, from periphery to center, are the lamina, the medulla and the lobula complex, which in flies and crabs includes the lobula and the lobula plate. These neuropils are organized in vertical columns corresponding to the ommatidial array. The columnar information is collected by relatively few wide-field tangential neurons that convey it downstream to different brain regions (Strausfeld and Nässel, 1981; Suver et al., 2016).

Semiterrestrial crabs are highly active visual animals. Each of their eyes is mounted at the tip of a vertical movable stalk and encompasses 360° of the visual field (Smolka and Hemmi, 2009). In many species, as the crab *Neohelice granulata* studied here, the eyestalks are set further apart likely to improve binocular vision (Collet, 1987; Berón de Astrada et al., 2012). Current studies in this crab indicate that it uses binocular depth vision during prey capture behavior (D.T., unpublished results). In addition, in crabs compensatory eye movements can be driven in a blind eye by visually stimulating the opposite eye with an optic flow, thus indicating a strong binocular coupling between the two eyes (Horridge and Sandeman, 1964). Altogether, these features establish the scenario for a potentially high degree of binocular processing as well as a convenient experimental model for its investigation.

Investigations on the crab *Neohelice* provided novel knowledge on the anatomical and physiological organization of the visual system of decapod crustaceans (Berón de Astrada et al., 2013; Medan et al., 2015; Bengochea et al., 2018). The studies led to the identification of a group of giant neurons from the lobula that are sensitive to object motion, which reflects many aspects of visually elicited defensive behaviors (for review, see Tomsic, 2016). By performing *in vivo* intracellular recordings, here we investigated the binocular properties of these neurons. We found that most of them exhibited binocular responses, although the degree of binocular responsiveness varied among neurons. Electrophysiological profiles indicated that neurons were recorded from their input side or their output side, likely corresponding to centripetal and centrifugal lobula neurons, respectively. This interpretation is supported by differences in response latency and by morphological characteristics of the neurons. Simplified model circuits of interocular connections are proposed to explain our main findings.

Materials and Methods

Animals

Animals were adult male *Neohelice granulata* crabs 2.7–3.0 cm across the carapace, weighing ~17 g, collected in the rías (narrow coastal inlets) of San Clemente del Tuyú, Argentina. The crabs were maintained in plastic tanks filled to 2 cm depth with artificial seawater prepared using hw-Marinex (Winex), salinity 10–14%, pH 7.4–7.6, and maintained within a range of 22–24°C. The holding and experimental rooms were kept on a 12 h light/dark cycle (lights on 7:00 A.M. to 7:00 P.M.) and the experiments were run between 8:00 A.M. and 7:00 P.M.

Visual stimuli

Computer-generated visual stimuli were projected on two computer screens (Samsung S20C300L) placed 99° to each other to cover the frontolateral sides of the animal (Fig. 1*A*). The crab was located equidistant to the screens, at a distance of 26.5 cm. The screens arrangement was housed inside a Faraday cage with opaque covers to prevent outside visual stimuli from reaching the animal. Visual stimuli were generated with a single PC, using commercial software (Presentation 5.3, Neurobehavioral Systems). The stimulus image generated by the PC was first split and then sent to a switcher for selecting between the two screens. The selector and other control systems used during the experiments were located outside the Faraday cage. In this way, the experimenter could choose which screen showed the stimulus at any time without distressing the animal.

To reversibly separate the visual field between the eyes while preventing the mechanical instability for intracellular recording that would result from manually attaching and removing pieces of hardware to the animal, we used the following procedure (Fig. 1). A piece of opaque soft rubber carved to fit the midline dorsal contour of the crab carapace was attached to the lower edge of a large rectangular piece of black cardboard. This piece, held from the roof of the cage, could be moved up and down to completely separate the visual field between the eyes (Fig. 1*A*). The vertical motion was operated by a step motor device, which allowed to gently approach the partition adjusting the soft carved piece to the animal dorsal contour (Fig. 1*B*). Experiments were initiated with the partition in the up or down position in balanced number.

Using the visual field partition the animal could see the stimulus moving on the left side only with the left eye. Therefore, these experiments allowed us to test whether neurons recorded from the right optic lobe (ipsilateral side) were capable of responding to contralateral stimulation by information conveyed from the contralateral eye. However, they did not provide information on whether neurons from the right optic lobe could also respond to contralateral motion by seeing the stimulus with the ipsilateral eye alone. To address this, we performed additional experiments where binocular and monocular conditions were attained by a different procedure, that consisted in reversibly covering the contralateral eye with a small cap made of aluminum foil (Fig. 1*C*). While recording from a cell in the right optic lobe, the cap was put on and taken off from the left eyestalk by gently handling it with one pair of tweezers.

Visual stimuli consisted of a black bar (4 × 21 cm; retinal subtended angle at the center of the screen 8.6°×43.3°) moving over a white background in the right or left screen. The stimulus was presented separately or simultaneously on the two screens, moving rightward, leftward, downward, or upward, always perpendicular to its major axis, at a speed of 11 cm/s. The distances covered in horizontal and vertical translations were 37 and 17 cm (spanning arcs of 69.8° and 35.6°, respectively). The size and speed was chosen based on previous studies showing that this stimulus effectively evoked behavioral responses in the laboratory (Scarano and Tomsic, 2014). To avoid the effect of appearing and disappearing from behind the borders of the screen, the stimulus started and ended its trajectory from positions separated 1 cm from the screen borders. Stimulus images were present stationary for 30 s before movement onset. The order of stimulation (screen and movement direction) was randomized and the intertrial interval was 1 min to curtail habituation.

Electrophysiology

Intracellular recordings were performed in the optic lobes of intact living animals according to methods previously described (Berón de Astrada and Tomsic, 2002). Briefly, the crab was firmly held in an adjustable clamp and the eyestalks were fixed to the carapace using a small metal corbel glued with cyanoacrylate (LOCTITE super glue), at an angle ~50° from the horizontal line, which corresponds to their normal seeing position (Berón de Astrada et al., 2012; Fig. 1*B–D*). In crabs, the movements of the two eyestalks are highly coupled and intended for compensating optic flow (Nalbach et al., 1993), but have little or no role in object tracking (Barnes and Nalbach, 1993), which is achieved by the rotation of the whole animal's body (Land and Layne, 1995). Yet, the procedure of immobilizing the eyestalks, required to perform intracellular recordings, may lead to certain misalignment of the eyes affecting to some extent the receptive field of binocular neurons. With this caveat in mind, we pay attention to fix the eyestalks as close as possible to their natural position. To access the optic ganglia we removed a small section of cuticle (~500 μm in diameter) from the tip of the eyestalk without causing damage to the ommatidia area and advanced a glass microelectrode through the opening in the cuticle (Fig. 1*D*,*E*). Microelectrodes (borosilicate glass;

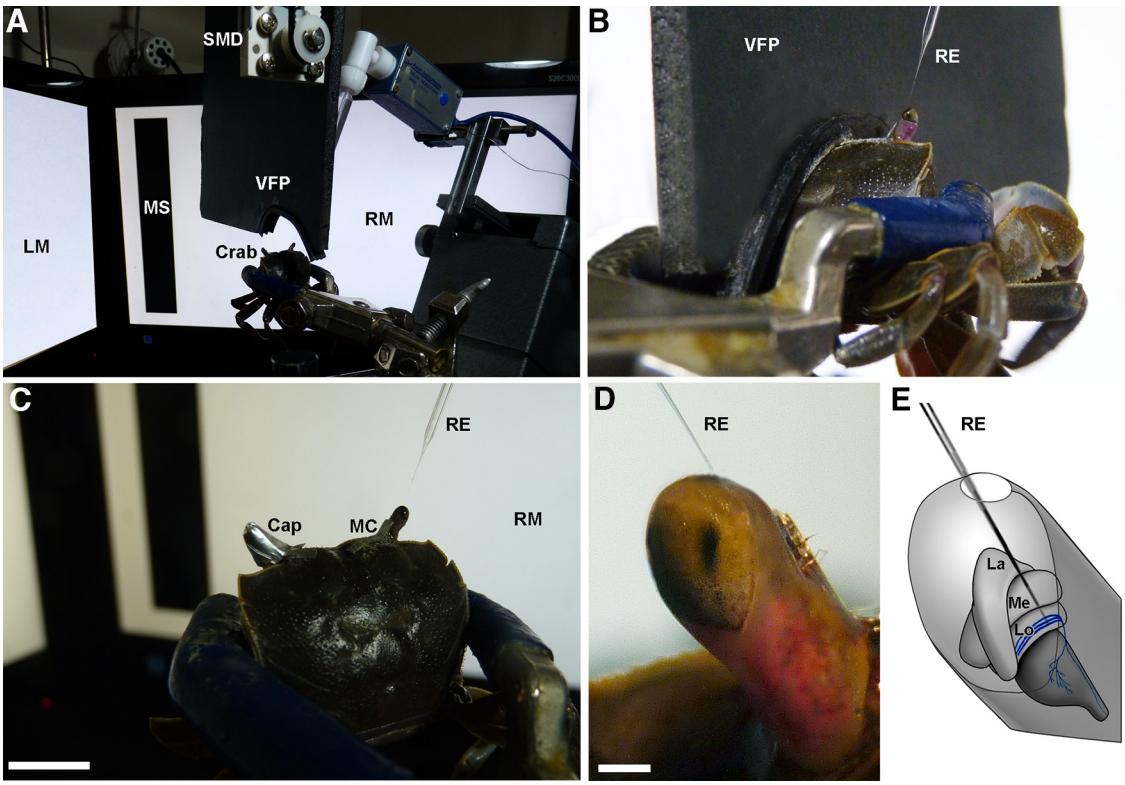

Figure 1. Experimental set up and methods. The crab was held in an adjustable clamp and the eyestalks were glued (cyanoacrylate) in the typical seeing position (50° from the horizontal line) using a metal corbel (MC). ***A***, A crab inside the setup facing the two screen monitors. LM, Left monitor; RM, right monitor; MS, motion stimulus. During intracellular recording from a neuron, a visual field partition (VFP) could be moved up and down by a step motor device (SMD) remotely controlled. ***B***, When lowered, the VFP prevented each eye from seeing the motion stimulus presented on the opposite side. RE, Recording electrode. ***C***, In another series of experiments a cap was used to cover and uncover the contralateral eye while recording from a neuron. ***D***, Anterior view of a right eye. The RE is advanced through a small opening made in the cuticle at the tip of the eyestalk (illustrated in ***E***). ***E***, Representation of the optic lobe inside the eyestalk, with the retinotopic neuropils. La: Lamina; Me, medulla; Lo, Lobula. Inside the lobula is represented a LG neuron of the type recorded in the present study. Scale bars: ***C***, 1 cm; ***D***, 500 μm.

1.2 mm outer diameter, 0.68 mm inner diameter), were pulled on a Brown-Flaming micropipette puller (P-97, Sutter Instruments) yielding tip resistances of 40–60 MΩ when filled with 3 M KCl. A bridge balance amplifier was used for intracellular recordings (AxoClamp 2B, Molecular Devices). Signals were digitized at 10 kHz (Digidata 1320, Molecular Devices) and recorded with Clampex for off-line analysis using pClamp 9 (Molecular Devices).

A large series of studies recording and staining neurons in *Neohelice*'s optic lobe consistently showed that wide-field elements exhibiting a strong response to motion and a weak or even absent response to a light flash, are large tangential neurons from the lobula (Berón de Astrada et al., 2002, 2013; Medan et al., 2007). In fact, a rapid simple test with a flash of light and with a manually moved screen around the crab, allows to recognize wide-field motion-sensitive neurons that, when stained, always prove to be from the lobula. Therefore, after impaling a cell, we performed this rapid test and if the neuron showed a clear-cut preference for motion stimulation the experiment began. Because of their size and location, wide-field motion-sensitive elements have been generically called lobula giant (LG) neurons (Fig. 1*E*). Four different classes of LG neurons have been morphologically identified and physiologically characterized, two presenting monostratified arborizations in the lobula, MLG1 and MLG2, and two with bistratified arborizations, BLG1 and BLG2 (Medan et al., 2007). The systematic correspondence found between the morphology and certain physiological features within each class, that includes intrinsic neuronal properties and stimulus preferences, make it usually possible to recognize the LG class by the neuron's electrophysiological profile (Medan et al., 2007). Briefly, MLG1 neurons are easy to distinguish from the other LG neurons because they have a comparatively smaller receptive field (~120°), lack spontaneous firing and show no mechanosensory response (Medan et al., 2015). Neurons of the class BLG2 have a characteristic spontaneous activity presenting bursts of 2–5 spikes and a response to looming stimuli that is clearly different from that of the other three LG classes (Tomsic et al., 2017). Neurons of the classes MLG2 and BLG1 both present a regular spontaneous activity, mechanosensory response, and sensitivity for looming stimuli. Although they show some differences in terms of receptive field and stimulus preferences (Medan et al., 2007), a clear distinction between these two classes often requires morphological identification. None of the identified LG classes exhibits directional preference (Medan et al., 2007).

Once a neuron was impaled and its object motion response was confirmed, a black curtain was lowered to prevent uncontrolled visual stimulation and to leave the animal undisturbed for 10 min before the experiment began. All intracellular recordings were performed at resting membrane potential. If resting potential changed >10% the experiment was ended. Because recordings were performed from the right lobula, the right side is referred as ipsilateral.

Neuroanatomy

Individual LG staining. In the present study, the long time required for evaluating the neuronal responses to all stimulus conditions precluded us to stain and morphologically identify the neurons. The physiological results, however, prompted us to reanalyze the images of stained LG neurons from our database of previous studies (Medan et al., 2007), focusing on morphological details not accounted before. The staining procedure and tissue preparation were described previously (Medan et al., 2007, 2015). Optic ganglia were imaged as whole mounts and scanned at 2–5 μm intervals with a confocal microscope equipped with a Helium/Neon laser (Olympus, FluoView 1000, FV1000BX 61WI; objective lens UMPlanFI 10×/0.3 w and UplanFI 20×/0.5 s). Images, saved as 3D stacks, were adjusted for brightness and contrast, and illustrations were

obtained by merging the individual serial sections with ImageJ 1.48d (NIH).

Mass staining of lobula neurons. LG neurons project their axons to the midbrain exiting the eyestalks through the protocerebral tract, but intracellular stainings have failed to reveal their projections beyond the tract. In an effort to disclose the central projections, we performed local applications of fluorescent dextran crystals in the lobula (dextran-AlexaFluor 488 and dextran-AlexaFluor 680; 3000 MW, Invitrogen). To this aim, we held the crab in an adjustable clamp, cemented the eyestalk to the carapace and cut a small hole in the eyestalk cuticle. We next applied each dye with a fine glass probe inserted in the cuticle hole, which was gently rotated and removed after 5–10 s leaving a spot of dye. Crystals were let to diffuse for 3–4 h, then the crab was anesthetized on ice and the two optic lobes and the supraesophageal ganglion were dissected and fixed overnight in PFA 4%, washed with PBS, dehydrated in ethanol series and cleared in methyl salicylate (Berón de Astrada et al., 2011). Images were obtained and processed as described in the previous paragraph.

Data analysis and statistics

A complete experiment comprised the bar moving in four directions, in each screen independently and in both screens simultaneously, with and without the visual field partition, i.e., 24 stimuli delivered in ~35 min of intracellular recoding. We were able to complete the whole stimulation series in 34 neurons from 34 animals. In eight cases, a second series of stimulation could be finished. In these cases, repeated responses to the same condition of stimulation showed to be highly consistent. Only one response per stimulus condition was used in the analyses. During the recording time the animal sporadically moved its legs, which sometimes caused loss of the cell impalement before the end of the experiment. Yet, experiments in which data with binocular and monocular responses to both sides of stimulation could be obtained for at least one motion direction were included in the general analyses. Detailed analyses were done on responses to the rightward moving stimulus, because it was the direction for which we obtained monocular and binocular responses to ipsilateral and contralateral stimulation in a larger number of neurons (42 neurons).

To quantify the responses of the neurons in the natural binocular condition to stimuli moved in the contralateral or the ipsilateral side we calculated an index of side preference (ISP). The ISP compared the number of action potentials (AP) elicited by ipsilateral versus contralateral motion stimulation:

$$ISP = \frac{number\ of\ AP\ ipsi - number\ of\ AP\ contra}{number\ of\ AP\ ipsi + number\ of\ AP\ contra}$$

This index varies from −1 to 1, corresponding to exclusive contralateral or ipsilateral preference, respectively. Because the 360° visual field of the crab's eye (Berón de Astrada et al., 2012) make possible that neurons respond to contralateral stimulation seen by the ipsilateral eye, the ISP is not a binocularity index but an index to characterize the spatial side preference of the neurons.

To determine the contribution of each eye to the responses obtained under the binocular condition, we assessed the responses of each neuron to contralateral or to ipsilateral stimulation with or without the central visual field partition. This allowed us to calculate an index of monocular contribution (IMC) for each neuron, which is a normalized ratiometric index analogous to those used to describe binocular circuits in mammals and other species (Hubel and Wiesel, 1962; Ramdya and Engert, 2008). The IMC compared the number of AP elicited under a binocular condition versus a monocular condition:

$$IMC = 1 - \frac{number\ of\ AP\ binocular - number\ of\ AP\ monocular}{number\ of\ AP\ binocular + number\ of\ AP\ monocular}$$

This index varies from 0 to 2, with values near 0 reflecting a null monocular response, values ~1 reflecting similar monocular and binocular responses, and values near 2 reflecting an exclusive monocular response that is suppressed under the binocular condition. Given the natural variation of activity expected in central neurons recorded in an intact and awaken animal, we followed a standard parsimonious criteria used in related studies to define a response difference (Livingstone and Conway, 2003; Ramdya and Engert, 2008). According to this, response differences <50% of elicited spikes were considered similar responses.

To measure the response latency we considered the time elapsed between the beginning of stimulus motion and the first elicited spike. We only computed latency data for recordings where this measure could be reliably established.

Only neurons that responded with a minimum of 10 spikes to at least one stimulus condition were included for analyses. One- or two-way repeated-measures ANOVA with side of stimulation (contralateral, ipsilateral, bilateral) and condition (binocular, monocular) as factors of analysis were performed to disclose response differences. We used Tukey or Bonferroni's multiple-comparisons *post hoc* tests. The extra sum of squares *F* test was used to compare the best-fit values for the IMC distribution parameters. A paired Student's *t* test was used to compare the latencies difference. All statistical analyses were performed with GraphPad Prism software. All data are presented as the mean ± SEM. In the figures, $*p < 0.05$, $**p < 0.01$, and $***p < 0.001$. All experimental protocols were performed in accordance with relevant guidelines and regulations of the Universidad de Buenos Aires.

Results

LG responses to contralateral, ipsilateral, and simultaneous bilateral stimulation

Our initial analysis comprised 104 neurons recorded from 78 crabs that responded to bar motion. To later assess the binocular properties of these neurons, we first investigated their ability to respond to stimuli presented on the ipsilateral (the recording side) and the contralateral side independently, or on both sides simultaneously (bilateral). Figure 2*A* illustrates a variety of responses found among the recorded neurons. The top traces are from a neuron that only responded to the stimulus presented on the ipsilateral screen, the middle traces are from a neuron that only responded to the stimulus presented on the contralateral screen, and the bottom traces are from a neuron that responded to the stimulus moved on both sides. On average, the number of elicited spikes by ipsilateral and by bilateral stimulation was similar, and higher than that elicited by contralateral stimulation (repeated-measures one-way ANOVA, $F_{(2,202)} = 10.24$, $p < 0.0001$; Tukey's multiple-comparison test, contralateral vs ipsilateral: $p < 0.0001$, contralateral vs bilateral: $p = 0.0076$; ipsilateral vs bilateral: $p = 0.3486$; Fig. 2*B*). To take into consideration the individual cell responses we applied an ISP (Fig. 2*C*; see Materials and methods). The frequency distribution of the ISP shows that most recorded neurons have values comprised between ±0.33, meaning they responded rather similar to the stimulus presented on one or the other side. A few neurons however, showed ISP beyond these values, indicating they responded with at least 50% more spikes to the stimulus presented on one side than on the other. The individual ISP distribution of the 104 neurons (red square dots) shows that the larger number of neurons with a marked side preference had positive values, meaning they responded more to ipsilateral than to contralateral stimulation. In fact, six cells responded exclusively to the stimulus moved on the ipsilateral side (ISP = 1), whereas only one cell responded exclusively to the contralateral side (ISP = −1). Neurons with the highest ISP absolute values (i.e., with receptive fields limited to a single screen), were identified by physiological criteria (see Materials and Methods) as MLG1 neurons (Medan et al., 2007, 2015). Because of their restricted lateral visual field, these seven cells were excluded from further analyses.

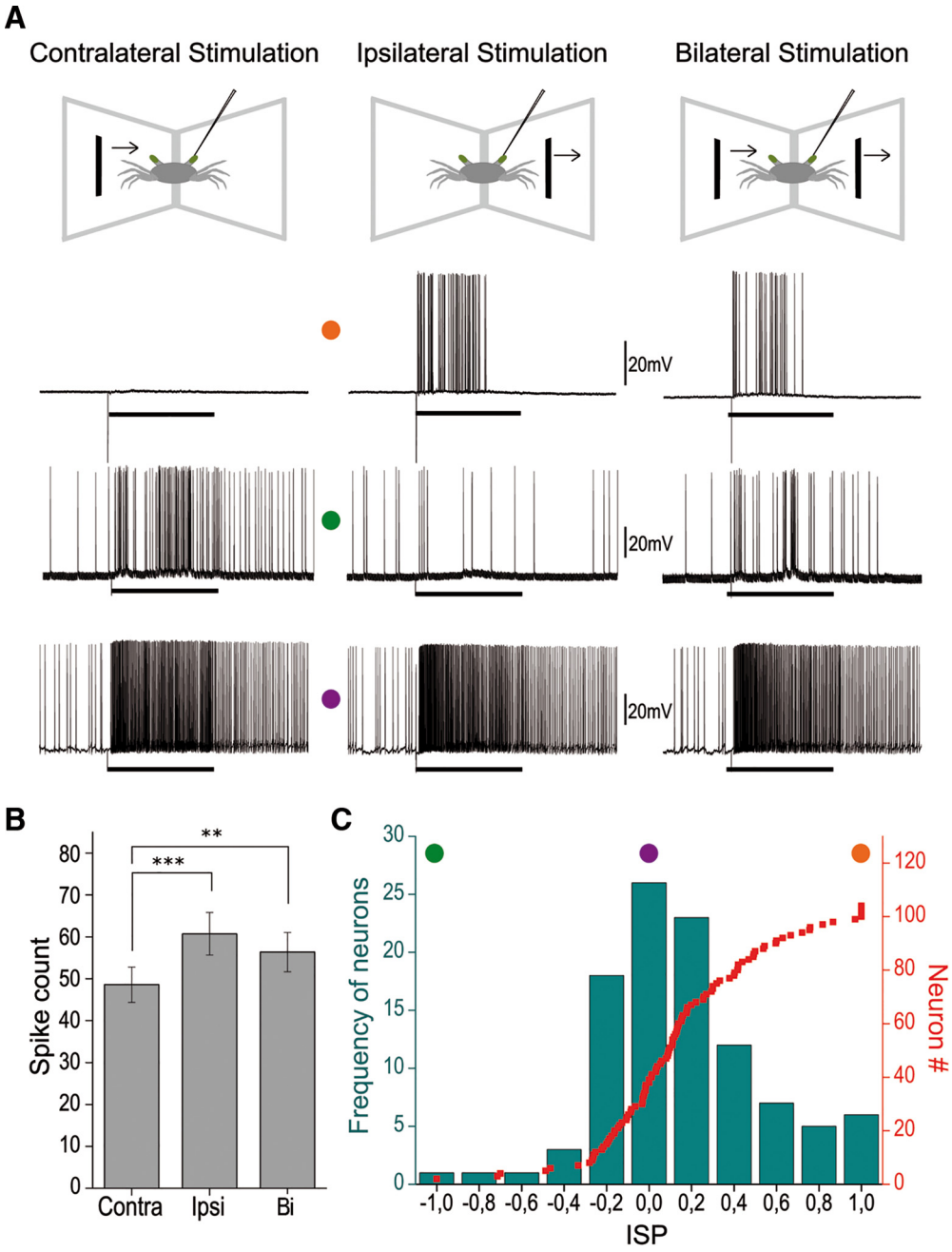

Figure 2. Evaluation of side preferences in individual lobula neurons. ***A***, Top row, schematic representation of the experimental setup showing the stimulation screens and the living crab with the sharp electrode positioned to record from the right optic neuropils within the eyestalk (not on scale). On the left, the stimulus is presented in the opposite side of the recording (contralateral stimulation), on the center, the stimulus is presented ipsilateral to the recording side, and on the right the stimulus is simultaneously presented on both screens (bilateral stimulation). In all cases, the bar moved rightwards for 3.36 s (black horizontal bar under recordings). Top traces are from a neuron that responded only to ipsilateral stimulation, middle traces from a neuron that responded to contralateral stimulation, and bottom traces from a neuron that responded to either side equally. ***B***, Mean number of elicited spikes in the same group of neurons to contralateral stimulation (Contra), ipsilateral stimulation (Ipsi), or bilateral stimulation (Bi). ***C***, Frequency distribution of the ISP (index of side preference) values of the recorded neurons. Red square dots represent the individual ISP values of 104 neurons. Purple, orange and green dots represent the position in the histogram of the corresponding neuron's traces depicted in ***A***. Bars show mean ± SEM. $^{**}p < 0.01$, $^{***}p < 0.005$.

Binocular versus monocular LG responses to contralateral and ipsilateral stimulation

From the 97 neurons that responded to motion stimulation on both sides, we succeeded to record the binocular and monocular responses (i.e., with and without the visual field partition between the eyes, Fig. 1*A*,*B*) to contralateral and ipsilateral stimulation for the rightward moving bar in 42 cells. An analysis of the mean number of elicited spikes of these neurons (Fig. 3*A*), revealed a significant effect of the stimulation side, but not of the binocular and the monocular condition or the side by condition interaction (repeated-measures two-way ANOVA, Side: $F_{(2,82)} = 15.01$, $p < 0.0001$; Condition: $F_{(1,41)} = 1.62$, $p = 0.21$; Side × Condition: $F_{(2,82)} = 2.48$, $p = 0.09$). Therefore, aside of a lower response to contralateral stimulation (Tukey's multiple-comparison test: contralateral vs ipsilateral $p < 0.0001$), binocular and monocular responses were equivalent. The same analysis performed on responses to the leftward moving bar ($n = 35$) rendered a similar result, i.e., a smaller response to contralateral

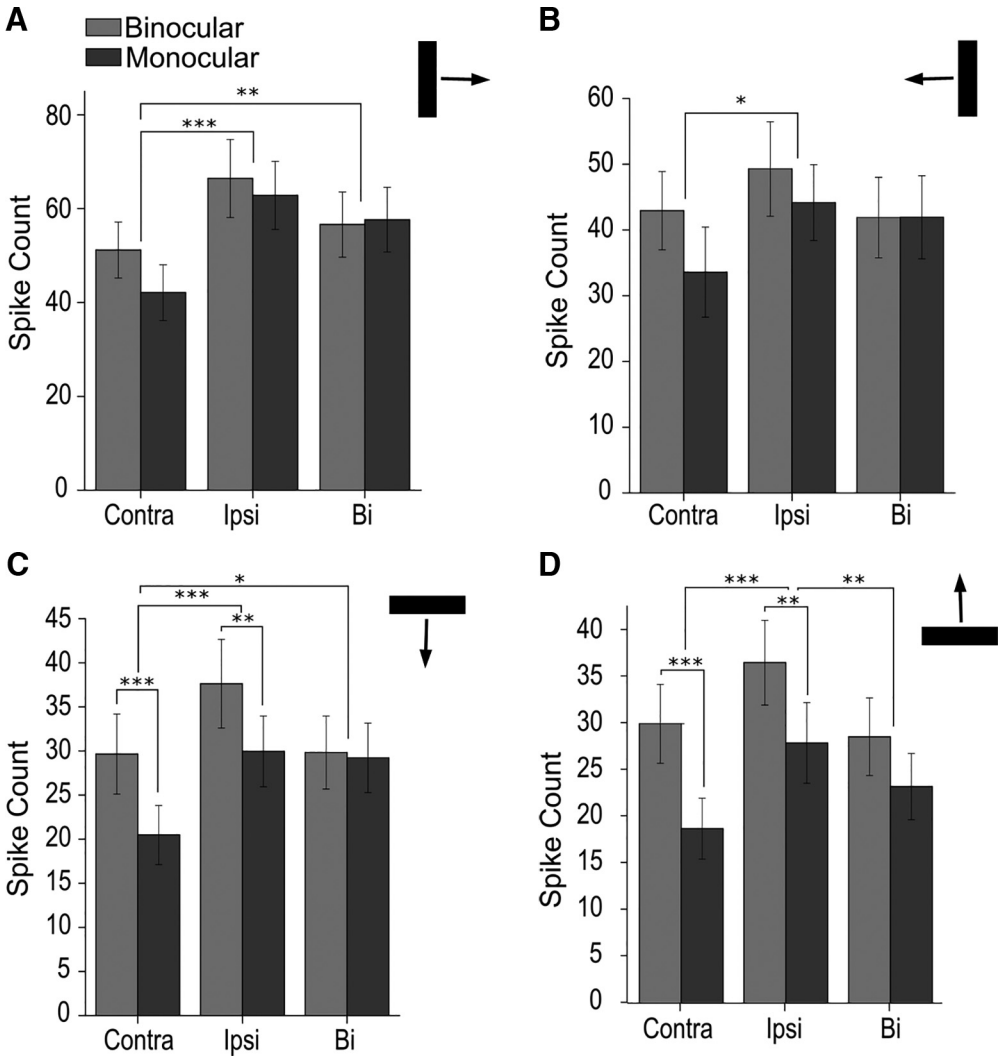

Figure 3. Average binocular and monocular responses to contralateral, ipsilateral, and bilateral stimulation with a bar moving in four different directions. Mean response intensity to ipsilateral (Ipsi), contralateral (Contra) or bilateral stimulation (Bi) for a bar moving rightward ($n = 42$; ***A***), leftward ($n = 35$; ***B***), downward ($n = 38$; ***C***), and upward ($n = 37$; ***D***). Light gray bars, binocular condition; dark gray bars, monocular condition. Bars show mean ± SEM. *$p < 0.05$, **$p < 0.01$, ***$p < 0.005$.

stimulation (Tukey's multiple-comparison test: contralateral vs ipsilateral $p = 0.019$) and no difference between binocular and monocular responses (Fig. 3*B*). Therefore, results from the horizontally moving bar show, for both directions, that a great deal of motion information is conveyed from the contralateral eye. When the analysis was performed on the responses to the vertically moving bar the main result was confirmed, i.e., neurons exhibited clear monocular responses to contralateral stimulation (Fig. 3*C*,*D*). However, the monocular responses were significantly smaller than the binocular responses, both for downward motion (Bonferroni's multiple-comparison test: $p < 0.0001$ and $p = 0.0016$ for contralateral and ipsilateral stimulation, respectively, $n = 38$; Fig. 3*C*), as well as for upward motion (Bonferroni's multiple-comparison test: $p = 0.0002$ and $p = 0.0054$ for contralateral and ipsilateral stimulation, respectively, $n = 37$; Fig. 3*D*).

The analyses of averaged responses provided a general picture of the magnitude of visual information conveyed to the lobula from the contralateral eye. However, not all the neurons responded in the same way. Figure 4*A* introduces the variety of responses that we recorded in different neurons to the right moving bar. Based on their differential responses to the distinct conditions of stimulation, neurons were classified within different categories (explained in detail below). Figure 4*B* shows the category label together with a conceptual scheme of the input pathways that can account for the responses observed in each neuron on the left.

To evaluate the contribution provided by the contralateral and by the ipsilateral eye to binocular responses of contralateral and ipsilateral stimulation in each neuron, we applied an IMC. This and further detailed analyses were performed on the responses to the right moving bar (see Materials and Methods). Figure 5*A* shows the frequency distribution of the IMC for contralateral and ipsilateral stimulation (IMCc and IMCi, respectively). The distribution of IMCi is centered on value 1, with most cells comprised between 0.67 and 1.33, which corresponds to differences between the binocular and the monocular condition of <50% in the number of elicited spikes. The distribution of IMCc is also centered on value 1, but with a different Gaussian distribution (extra sum-of-squares F test: $F_{(3,16)} = 8.58$, $p = 0.0013$), and a considerable number of cells showing values <0.67, i.e., neurons in which the sight from the contralateral eye elicited negligible responses. In these cells the response measured in the binocular condition must be mostly accounted for by in-

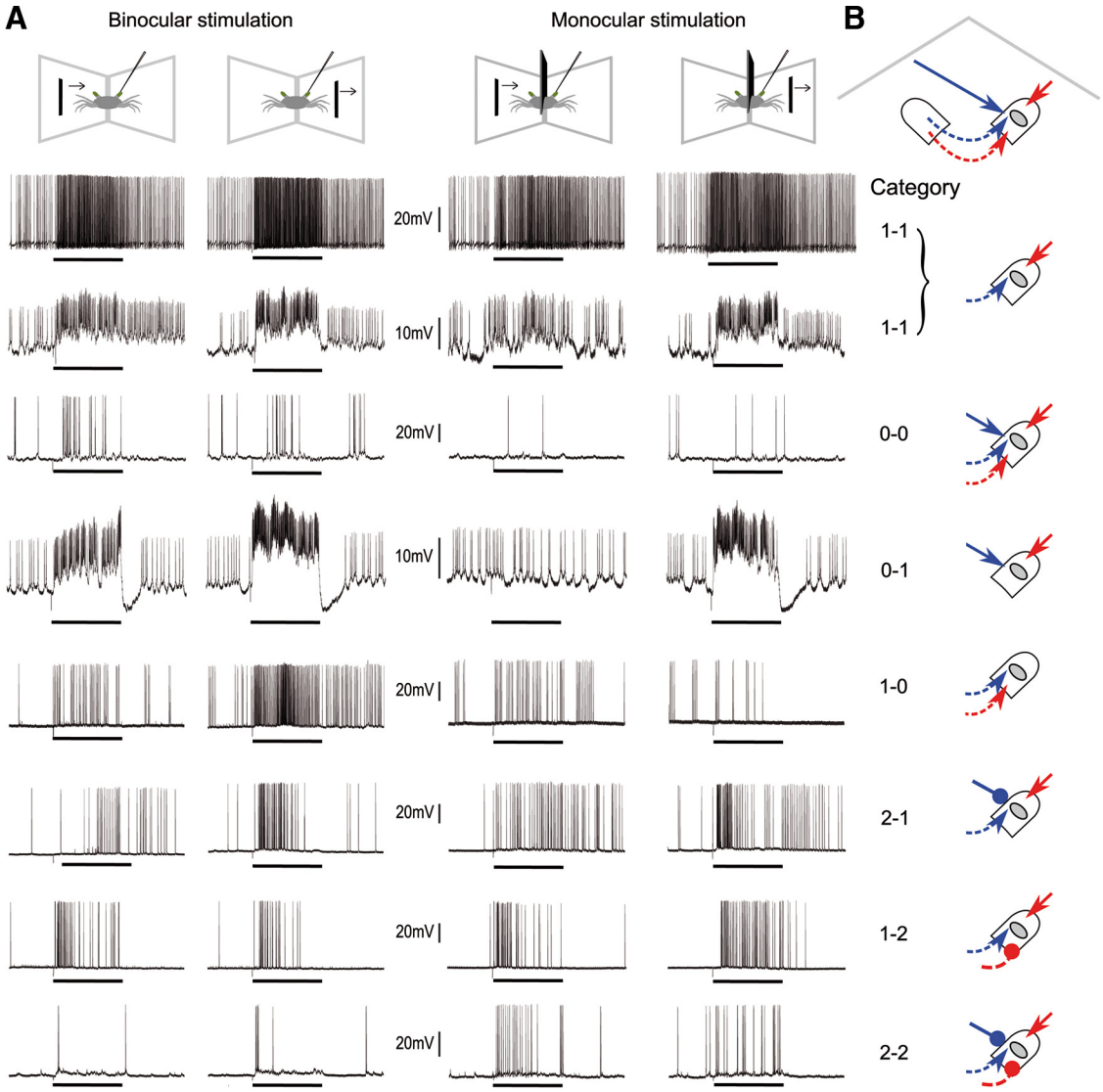

Figure 4. Variety of responses among LG neurons to ipsilateral or to contralateral stimulation under the binocular or the monocular conditions. ***A***, Examples of LG neurons (each row a single neuron) corresponding to the different categories (from 0-0 to 2-2) defined by the IMCc and IMCi described in the text. Because category 1-1 is the most frequent (Fig. 5*B*), two examples are shown. In the left two columns, crabs have seen the stimulus in a binocular condition. In the right two columns, a division between the eyes only allowed crabs to perceive the stimulus in a monocular fashion. ***B***, The top scheme presents the general reasoning used to interpret each one of the response categories depicted below. Solid lines stand for information entering through the ipsilateral eye and dashed lines represent information entering through the contralateral eye. Red and blue colors are for the stimulus presented on the ipsilateral and the contralateral side, respectively. The gray oval represents a recorded LG neuron. Arrowed and circular terminals represent excitatory and inhibitory input pathways, respectively. Each scheme represents the combination of pathways that can account for the responses of the corresponding neuron aligned at the left. Further explanations are in the section Binocular versus monocular LG responses to contralateral and ipsilateral stimulation.

formation incoming from the ipsilateral eye. Figure 5*B* shows the IMCc and the IMCi for each cell. According to the criteria of 50% response difference described in Materials and Methods, the combination of both indexes defines nine possible categories of binocular interaction. Each category was labeled with a two-digit code, the first digit reflecting the IMCc and the second the IMCi. Each digit could get the value 0, 1, or 2. Zero comprises the range of monocular responses where intensity was weaker (<50%) than the corresponding binocular responses, 1 includes the range of monocular responses where intensity was not substantially different from the binocular responses, and 2 includes monocular responses where intensity was stronger (>50%) than the binocular responses. The nine categories are separated by dotted lines in Figure 5*B* and can be further described as follows:

Category 1-1

Includes most of the recorded neurons (41%) and corresponds to neurons with similar monocular and binocular responses, both for contralateral and for ipsilateral stimulation. Their responses to contralateral and ipsilateral stimulation could be purely accounted for by monocular vision from the contralateral and ipsilateral eye, respectively. Binocular vision does not boost these responses (Fig. 4, traces 1-1 and scheme).

Category 0-0

Includes neurons with substantial response elicited only under binocular vision. Responses to contralateral and to ipsilateral stimulation require integrating inputs from both eyes. Responses in monocular visual conditions are negligible (Fig. 4, traces 0-0 and scheme).

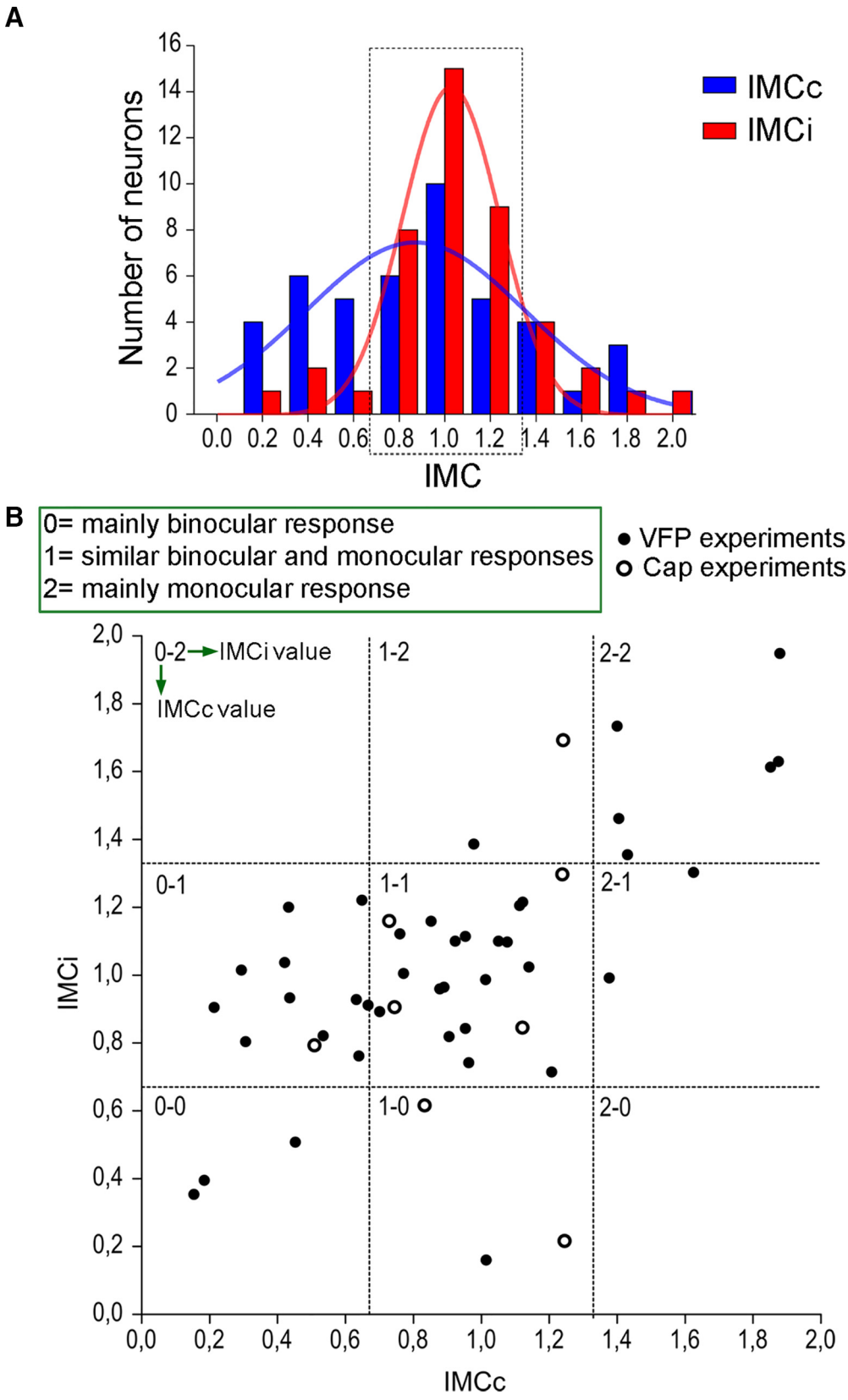

Figure 5. Categories of LG neurons based on monocular and binocular responses to ipsilateral and contralateral stimulation. ***A***, Histogram showing the distribution of neurons according to their IMC values (see text). Blue bars, IMC contralateral, Gaussian best-fit values: Amplitude: 7.53; Mean: 0.86; SD: 0.48. Red bars, IMC ipsilateral, Gaussian best-fit values: Amplitude: 14.30; Mean: 1.025; SD: 0.21. Most cells have IMC values within 0.67 and 1.33 (dashed rectangle), meaning that their binocular and monocular responses are not different (see Materials and Methods). ***B***, Scatter plot showing the IMCc and IMCi of each cell from the experiments with the visual field partition (solid circles). Open circles show the IMC values of neurons from the cap experiments (see text). Dashed lines separate the nine categories, labeled from 0-0 to 2-2 as described in the section Binocular versus monocular LG responses to contralateral and ipsilateral stimulation.

Category 0-1
Contains the second most recorded type of neurons (27%), stands for neurons with poor or no response to contralateral monocular stimulation but similar monocular and binocular responses to ipsilateral stimulation. Therefore, responses to both sides of stimulation would be mostly achieved by inputs from the ipsilateral eye alone (Fig. 4, 0-1).

Category 1-0
Includes neurons with similar monocular and binocular responses to contralateral stimulation, but with poor response to ipsilateral monocular stimulation. Therefore, responses to both sides of stimulation would be mostly achieved by inputs from the contralateral eye alone (Fig. 4, 1-0).

Category 2-1
Corresponds to neurons with similar monocular and binocular responses to ipsilateral stimulation, but weaker binocular than monocular response to contralateral stimulation. Responses to ipsilateral stimulation can be accounted for by monocular ipsilateral inputs alone. Responses to contralateral stimulation would be shaped by excitatory inputs from the contralateral side and inhibitory inputs from the ipsilateral eye (Fig. 4, 2-1).

Category 1-2
Corresponds to neurons with similar monocular and binocular responses to contralateral stimulation, but weaker binocular than monocular responses to ipsilateral stimulation. Here, responses to contralateral stimulation can be accounted for by monocular contralateral inputs alone. Binocular responses to ipsilateral stimulation would be reduced by inhibitory inputs from the contralateral eye (Fig. 4, 1-2).

Category 2-2
Comprises a considerable proportion of neurons (15%), which monocular responses are strongly inhibited under the binocular condition for both sides of stimulation. For ipsilateral stimulation, these neurons would receive excitatory inputs from the ipsilateral eye and inhibitory inputs from the contralateral eye, whereas for contralateral stimulation they would receive excitatory inputs from the contralateral eye and inhibition from the ipsilateral eye (Fig. 4, 2-2).

Finally, category 2-0 would comprise neurons with a higher monocular than binocular response to contralateral stimulation, and a weak monocular response to ipsilateral stimulation, whereas category 0-2 would comprise neurons with a higher monocular than binocular response to ipsilateral stimulation, and a weak monocular response to contralateral stimulation. We did not record any neuron fitting the last two categories.

The use of a partition to impede the binocular vision of the stimulus adopted in these experiments prevented us to assess the neuron's ability to respond to contralateral motion with information communicated only by the ipsilateral eye (with the partition the response to contralateral stimulation was provided by the contralateral eye). Therefore, we were unable to know whether the bilateral receptive field of a neuron is built on two complementary hemifields, i.e., a contralateral and an ipsilateral hemifield provided by the left and the right eye, respectively, or it contains an overlapped representation of the visual area through information conveyed by both eyes. To carry out a direct evaluation of the neuron's ability to respond to contralateral motion when the stimulus is seen by the ipsilateral eye alone, we performed 8 additional experiments using, instead of the visual field partition, a removable cap to cover the contralateral eye (Fig. 1*C*; see Materials and Methods). The mean spike response to contralateral stimulation elicited under this monocular condition was similar to the mean response elicited under the binocular condition (contralateral monocular: 47.25 ± 11.52, contralateral binocular: 50.87 ± 12.75). As expected, the monocular and binocular mean responses to ipsilateral stimulations were also similar (ipsilateral monocular: 42.87 ± 12.01, ipsilateral binocular: 50.25 ± 13.55). An individual analysis based on the IMCc showed that, with only one exception, the IMCc value of all neurons fell in category 1 (Fig. 5*B*, open symbols). Therefore, almost all tested neurons responded to contralateral stimulation in the ipsilateral monocular condition as intensely as they do in the binocular condition. These results show that the monocular receptive field of LG neurons extends to the contralateral visual space. In this experiment, we did not evaluate the response under both the ipsilateral monocular condition and the contralateral monocular condition in the same neuron. Thus, it could be argued that we do not know whether these neurons processed information of the same visual area from the contralateral eye. However, the fact that the monocular ipsilateral visual field of all the eight tested neurons encompassed the ipsilateral and the contralateral visual area, in connection with the result of the previous experiment showing that most neurons received information of the contralateral visual field through the contralateral eye, strongly suggest that most LG neurons receive information from the same points in space through both eyes, i.e., that they process a moving target binocularly.

Ipsilateral and contralateral lobula neurons
In honeybees, lobula neurons sensitive to optic flow were found to integrate binocular information (DeVoe et al., 1982). These neurons present tangential neurites extending across the retinotopic mosaic of the lobula, which converge into an axon fiber that project contralaterally to arborize with a similar pattern in the opposite lobula. According to the electrical profiles of intracellular recordings, the authors concluded that some neurons were impaled near their synaptic input region, thus being ipsilateral elements, whereas other neurons were impaled in their terminal endings, thus being contralateral projecting elements. The first group was characterized by having: (1) spike discharges superimposed on depolarizations, (2) small spikes that did not reach zero potential, and (3) no undershoot or after hyperpolarization (AHP) at the end of spikes. The second group, on the other hand, was characterized by having: (1) large spikes that overshot or reached near zero potential, (2) undershot of resting potential after the spikes, and (3) no observable synaptic polarizations (DeVoe et al., 1982). A cursory inspection of the traces in Figure 4*A*, together with the bimodal distribution of spike amplitudes shown in Figure 6*A*, suggest that similar criteria can be applied to separate our recordings of lobula neurons in the crab. Figure 6, *B* and *C*, schematizes the reasoning and the criteria over the electrical response profile corresponding to a neuron recorded from its input side, i.e., an ipsilateral neuron, and on the profile corresponding to a neuron recorded from its output side, i.e., a presumably contralateral neuron. In a few neurons, the recorded traces did not comply with all the three aforementioned criteria for an exemplary presynaptic or postsynaptic recording site. For example, in Figure 4 the recording shown in the third row (0-0-labeled neuron) has considerably large spikes (68 mV), however, it was classified as postsynaptic because the spikes are on top of EPSPs, they do not exhibit an AHP and they do not overshoot zero potential (the resting membrane potential of this cell was −70 mV). On the other hand, the recording shown in the seventh

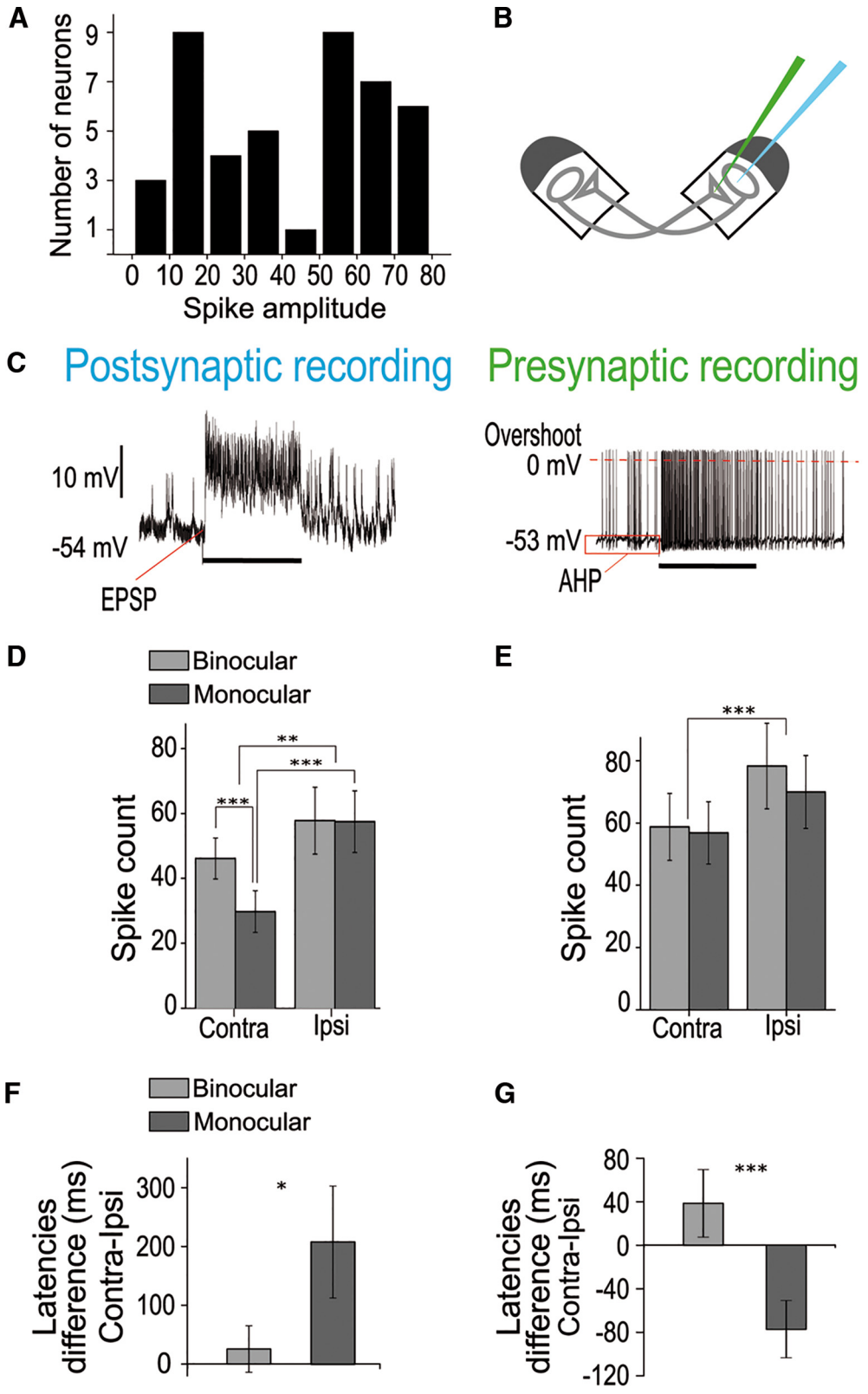

Figure 6. Presynaptic and postsynaptic-recorded neurons. ***A***, Frequency distribution of neurons according to the size of their action potentials. ***B***, Scheme representing a postsynaptic (light blue) or a presynaptic (green) recording from the lobula neuropil, that helps to interpret the following results. ***C***, Examples of two neurons that illustrate the main differences in the electrical profiles used as criteria to distinguish postsynaptic and presynaptic recordings. The black bar beneath the recordings stands for the 3.36 s of motion stimulation. ***D***, ***E***, Mean number of elicited spikes of postsynaptic neurons (***D***) and presynaptic neurons (***E***) to contralateral stimulation (Contra) or ipsilateral stimulation (Ipsi), in binocular (light gray bars) or monocular (dark gray bars) condition. ***F***, ***G***, Latencies response difference between contralateral and ipsilateral stimulation in binocular (light gray bars) or monocular (dark gray bars) condition for postsynaptic-recorded neurons (***F***) and presynaptic-recorded neurons (***G***). Bars show mean ± SEM. *$p < 0.05$, **$p < 0.01$, ***$p < 0.005$.

row (1-2-labeled neuron) does not exhibit an AHP, however, it was classified as presynaptic because there are no signs of EPSPs, the spikes are 77 mV high, and overshot zero potential. By applying these criteria to the recordings of the 42 neurons in which experiments to the right moving bar were completed, two of us independently coincided in judging 21 of them as recorded postsynaptically and 19 as recorded presynaptically, whereas two neurons could not be assigned to any category.

We then analyzed postsynaptic and presynaptic-recorded neurons separately, and compared the intensity of response to ipsilateral and contralateral stimulation in the binocular and the monocular conditions. Within the group of postsynaptic neurons (Fig. 6*D*), the overall response to contralateral stimulation was significantly smaller than to ipsilateral stimulation, confirming the preferential side effect previously described (repeated-measures two-way ANOVA, Side: $F_{(1,21)} = 8.41$, $p = 0.009$). There was no significant effect of the monocular versus the binocular condition $p = 0.149$, but a significant side × condition interaction $p = 0.0004$. *Post hoc* comparisons showed that contralateral monocular stimulation elicited significantly less spikes than contralateral binocular stimulation and ipsilateral monocular stimulation (Bonferroni's multiple-comparison test: $p < 0.0001$ and $p < 0.0001$, respectively), but no difference between the binocular and monocular responses to ipsilateral stimulation. These results indicate: (1) that the binocular response of postsynaptic-recorded neurons to contralateral motion is only partially built on input signals conveyed from the contralateral eye, and (2) that signals from the ipsilateral eye alone can fully explain the binocular response of these neurons to ipsilateral motion. Within the group of presynaptic-recorded neurons (Fig. 6*E*), except for the overall effect of side preference between responses to ipsilateral and contralateral stimulation (repeated-measures two-way ANOVA, Side: $F_{(1,18)} = 11.18$, $p = 0.004$), no other statistical differences were disclosed. Because these neurons are thought to have their input site on the contralateral lobula (or in the supraesophageal ganglion, as discussed discussion), their response to ipsilateral monocular stimulation (a stimulus that could not be seen by the contralateral eye) must have built on information received via ipsilateral LG neurons.

We then evaluated the difference of response latencies to contralateral and to ipsilateral stimulation for each neuron. As expected, under the binocular condition this difference was not statistically distinct from zero, neither in the postsynaptic ($t_{(18)} = 0.65$ $p = 0.53$) nor in the presynaptic ($t_{(15)} = 1{,}24$ $p = 0.23$) recorded group of neurons (Fig. 6*F*,*G*). However, the group of postsynaptic-recorded neurons showed a positive difference value in the monocular condition (i.e., longer latency for contralateral than for ipsilateral stimulation) that was significantly higher than that shown in the binocular condition (Fig. 6*F*; $t_{(18)} = 1.946$, $p = 0.034$). On the other hand, presynaptic-recorded neurons showed a negative value in the monocular condition (i.e., shorter latency for contralateral than for ipsilateral stimulation), which was significantly lower than that shown in the binocular condition (Fig. 6*G*; $t_{(15)} = 4.082$, $p = 0.0005$). These results are consistent with neurons having their input site in the ipsilateral and contralateral side, respectively.

Lobula neuron projections

The vast majority of LG neurons investigated in the present study proved to respond to motion stimulation presented to each eye independently, which demonstrates that a great deal of visual information transfer occurs between the two lobula neuropils. However, what is the anatomical evidence for this connection in the crab?

In previous studies we have consistently stained four types of LG neurons (Berón de Astrada and Tomsic, 2002; Medan et al., 2007), however, we never succeeded to follow their axons beyond the protocerebral tract. To partially cope with this limitation, here we performed massive stainings of the lobula using dextran-conjugated dyes, which proved to be a suitable method for disclosing neuronal projections in the crab (Berón de Astrada et al., 2011; Bengochea et al., 2018). Although massive staining prevents the identification of individual neurons, its local application within the lobula ensures that the stained projections arise from neurons in this neuropil. Figure 7, *A* and *B*, shows the stained projections within the supraesophageal ganglion in a preparation where the dye was applied into the left lobula (data not shown). The dye stained a considerable number of neurons, which axons run along the protocerebral tract. The projections arborize in different regions of the supraesophageal ganglion, most of them on the side of the dye deposit (Fig. 7*A*,*B*, white arrows). Some fibers traverse the brain running anterior or posterior to the central body to enter the opposite protocerebral tract. To follow these projections beyond the protocerebral tract, we looked for marks of staining in the contralateral optic lobe. Only in few occasions we were able to see some marks, but they were faint and restricted to the lower part of the lateral protocerebrum. Although the results are not conclusive on whether there are neurons that directly connect the two lobula neuropils, the presence of stained fibers that ascend the contralateral protocerebral tract supports this assumption.

By reanalyzing previously intracellularly stained LG neurons, we found that the elements of the class BLG1 described by Medan et al. (2007), present morphological features compatible with either postsynaptic or presynaptic specializations in the lobula (Fig. 7*C*–*G*). Figure 7*C* shows a BLG1 with the cell body clearly stained, whereas Figure 7*D* shows a similar neuron, but without cell body. From eight stained BLG1 neurons, five showed the presence of the soma in the recording side and three did not. In all cases, the presence of the soma was associated with slim ending branches (Fig. 7*F*), whereas its absence was associated with terminal swellings or varicosities (Fig. 7*G*) typical of presynaptic structures. In addition, the mean spike amplitude of the neurons with stained soma was smaller than that of neurons without it (10.8 ± 1.98 vs 53.33 ± 6.01, respectively; $p < 0.0001$). In one preparation (Fig. 7*E*), the intracellular dye injection of a BLG1 rendered 3 BLG1 stained neurons, one of these with a cell body and slim ending processes, and the other two without cell body and with varicosities in their terminals. These results indicate that: (1) there is more than one BLG1 per lobula, (2) there are efferent ipsilateral elements and afferent (most likely contralateral) elements, (3) the general branching patterns of these efferent or afferent elements are similar, and (4) there is dye coupling between these elements.

Simultaneous ipsilateral and contralateral intracellular recordings

The analysis of electrical profiles rendered a similar number of postsynaptic-recorded neurons (residing in the impaled lobula) and presynaptic-recorded neurons (presumably projecting from the opposite lobula). A classification further supported by the differences found in the response latencies. This, together with the anatomical data showed above, made tenable to attempt recording simultaneously from two LG neurons, one from each lobula, to explore their potential connections by means of intra-

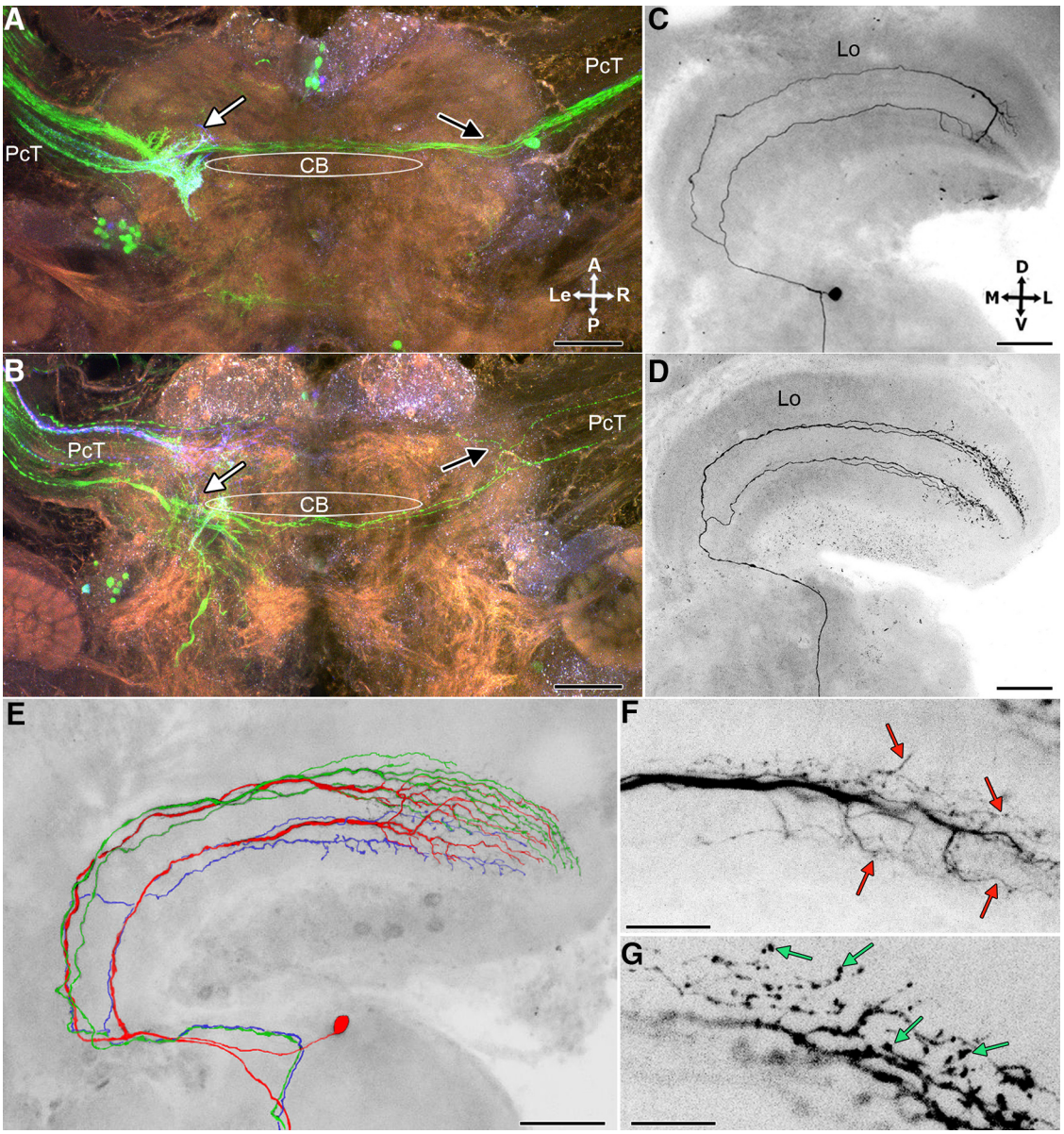

Figure 7. Anatomical support for binocular integration in the optic neuropils. ***A***, ***B***, Dextran-conjugated dyes were applied in the left lobula. Stained fibers from the left protocerebral tract (PcT) can be seen entering the supraesophageal ganglion. Figures show two confocal optical stacks of ~75 μm deep starting at different *z* positions. Two pathways traversing the brain anterior (***A***) or posterior (***B***) to the central body (CB) can be clearly observed. Many stained fibers exit the supraesophagic ganglion through the opposite PcT to enter the right eye. Most arborizations occur in the side of the brain where the dye was applied (white arrows), but some arborizations can be seen in the contralateral side as well (black arrows). ***C***, ***D***, Two examples of intracellular-stained neurons of the type BLG1 showing features compatibles with postsynaptic or presynaptic morphologies. The BLG1 in ***C*** shows the soma and fine branching processes consistent with a dendritic type of arborization. The BLG1 shown in ***D*** lacks the soma and presents arborization consistent with a terminal arbor, containing many varicose and baggy processes. ***E***, In this preparation three BLG1 neurons were costained, two of them showing presynaptic characteristics (green and blue) and one of them postsynaptic ones (red). Colors were added to distinguish the three neurons. A segment of the red and of the green neuron is enlarged in ***F*** and ***G***, respectively, where details of postsynaptic specializations (red arrows) and presynaptic specializations (green arrows) can be appreciated. Lo, Lobula; A, anterior; P, posterior; Le, left; R, right; M, medial; L, lateral; D, dorsal; V, ventral. Scale bars: ***A***–***E***, 100 μm; ***F***, ***G***, 20 μm.

cellular electrical stimulation. Performing simultaneous intracellular recordings from the two lobulae in a held but otherwise intact animal is a challenging experiment. Nonetheless, we succeeded to perform 17 dual stable recordings. Following the impalement of the two neurons and having confirmed that they both responded to motion stimulation in the two screens, we injected enough current into one neuron to make it fire at least threefold above its spontaneous rate, and observed the effects in the second neuron. In 11 experiments we were able to switch the procedure and made the second neuron to fire (Fig. 8), but in four experiments only one of the two neurons could be driven to increase the firing rate and in other two experiments the firing frequency could not be increased in any of the two neurons of the pair. Noteworthy, all the neurons in which the current injection failed to elicit spikes (or to affect the spontaneous spike rate), exhibited electrical profiles corresponding to a presynaptic recording. In these neurons, current injections must have been ineffective because of the long distance to the spike initiation zone, likely placed near the neuronal input site in the opposite lobula (or in the supraesophageal ganglion, see discussion). This observation is consistent with the notion that presynaptic-recorded neurons are afferent lobula elements.

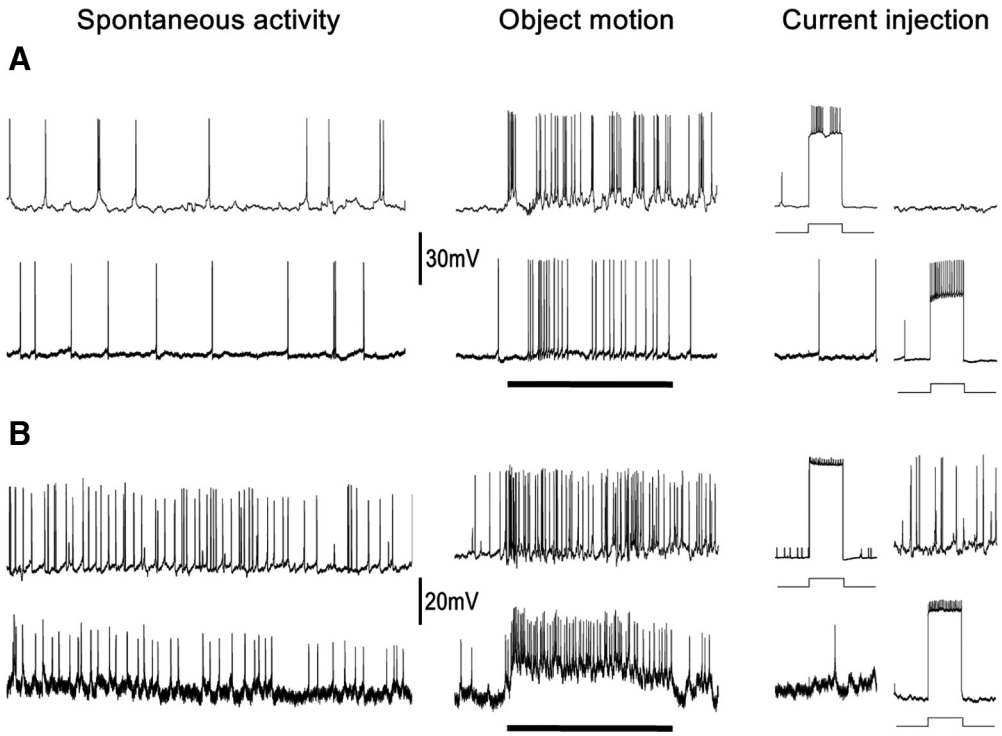

Figure 8. Simultaneous recordings of two LG neurons from opposite neuropils. ***A***, ***B***, Two examples of dual recording experiments of LGs. First column, Spontaneous activity. Second column, Response to a visual motion stimulus, which in this case moved during 2.2 s (black horizontal bar). Third column, Absence of evoked activity in one neuron (second and fourth trace) upon 500 ms step of depolarizing current sufficient to make the other neuron (first and third trace) to increase its spike frequency at least three times over the spontaneous activity. Fourth column, As in third column, but stimulating the other neuron.

When considering the experiments in which a neuron was indeed excited to fire or to increase its firing frequency by current injections, in no case we detected electrical changes in the membrane potential of the opposite recorded neuron that could be related to the spike trains evoked in the first neuron (Fig. 8).

Discussion

We investigated to what extent the binocular integration of object motion information occurs at the level of the optic neuropils of an arthropod. By recording the response of individual lobula giant neurons our main findings are as follows: (1) The vast majority of the recorded LG neurons proved to process object motion information perceived by the two eyes, although the contribution of each eye varied among neurons (Figs. 4, 5). (2) On average, the response to contralateral motion was weaker than to ipsilateral motion, in the binocular as well as in the monocular conditions (Fig. 3). Still, results highlight that the receptive field of most LG neurons encompasses an extensive part of the contralateral visual space. (3) On average, responses to ipsilateral stimulation and to simultaneous bilateral stimulation were similar in binocular as well as in monocular (Fig. 3) conditions. Thus, a second moving target seen either binocularly or bilaterally (i.e., with a visual field partition between the eyes) does not boost the response to a single target. (4) On average, there was no significant difference between binocular and monocular responses, either to ipsilateral or to contralateral stimulation with the horizontally moving bar (Fig. 3*A*,*B*). This may suggest that binocular responses are composed by information on ipsilateral motion acquired through the ipsilateral eye alone, and by information on contralateral motion acquired through the contralateral eye alone. In other words, that the neurons could receive information from different spatial areas from each eye, with the only purpose of extending their visual receptive field. Our cap experiments demonstrated that this is not the case, because all tested neurons proved to respond to the contralateral stimulus seen by the ipsilateral eye alone (Fig. 5*B*, open circles). These results show that most LGs receive overlapped information from both eyes, i.e., that they process information of a horizontally moving target binocularly.

Results with the vertically moving bar were slightly different. Although monocular responses to contralateral and to ipsilateral stimulation were manifest, they were significantly weaker than the corresponding binocular responses (Fig. 3*C*,*D*). The difference in the degree of binocular integration observed between horizontal and vertical moving bars is in line with the preference of LG neurons for horizontal rather than vertical motion (Medan et al., 2015) and with other adaptations to the flat world inhabited by these crabs.

Lobula neurons convey centripetal and centrifugal motion information

In an early study with the crab *Podophthalmus*, Wiersma et al. (1964) recorded responses of different types of motion-sensitive fibers from the optic tract to object motion perceived by the contralateral eye. They did not test responses to the contralateral and to the ipsilateral eye in the same neuron, so there was no information on whether the neurons responded to both eyes. Nonetheless, that study showed that axon fibers running along the protocerebral tract carry centripetal and centrifugal information of object motion. Because those recordings were made extracellularly, the morphology and location of the fibers remained unknown. More recently, intracellular recordings and staining in *Neohelice* revealed that the different classes of Wiersma et al.'s (1964) object-motion-sensitive fibers correspond to the LG neu-

rons that profusely arborize along tangential layers of the lobula (Berón de Astrada and Tomsic, 2002; Medan et al., 2007).

Inspired by the work of DeVoe et al. (1982), we separated our recordings of LG neurons in two groups. One showed an electrical profile compatible with a postsynaptic recording while the other with a presynaptic recording (Fig. 6). Under monocular stimulation, the group of postsynaptic-recorded neurons exhibited a shorter response latency to ipsilateral than to contralateral stimulation (Fig. 6*F*), supporting the notion that their input site is in the recording lobula (i.e., that they are ipsilateral neurons). Conversely, the group of presynaptic-recorded neurons showed a shorter latency to contralateral than to ipsilateral stimulation (Fig. 6*G*), indicating that their input site is in the opposite lobula (i.e., that they are contralateral elements recorded from their terminal projections in the ipsilateral side). These physiological interpretations were supported by anatomical data. First, massive dextran stainings of the lobula revealed the existence of two pathways connecting the brain regions between the two eyestalks (Fig. 7*A*,*B*). Second, intracellular-stained neurons of the class BLG1, showed morphological profiles compatibles either with postsynaptic or with presynaptic-recorded neurons (Fig. 7*C*–*G*).

Having demonstrated that LG neurons integrate information from both eyes, and that there appears to be cognate elements conveying motion information between the two lobulae, we attempted to investigate their connection by recording simultaneously from two LGs, one from each side. However, we were unable to detect any hint of electrical connections between opposite recorded neurons. Given the different LG classes and the still uncertain number of units within each class, a likely explanation for this failure is that we did not get to record from the right neuronal combination. Another possibility is that concerted inputs of several LG neurons from one side may be required to evoke responses in a neuron of the opposite side. Such input summation may take place in the lobula itself, as the costained elements in Figure 7*E* might suggest, or in bilateral regions of the supraesophageal ganglion where stained fibers from the lobula are seen to arborize (Fig. 7*A*,*B*, arrows). The presence of such relay stations along some of the pathways that convey information from the contralateral eye, in addition to explain the lack of success in our dual recording experiments, may be the reason why responses to contralateral stimulation are, on average, weaker than responses to ipsilateral stimulation (Fig. 3). These and other aspects of our main findings, such as the existence of inhibitory connections required to explain the response reduction observed under the binocular condition in some neurons (Fig. 4, last 3 recordings), are summarized in the schemes of Figure 9.

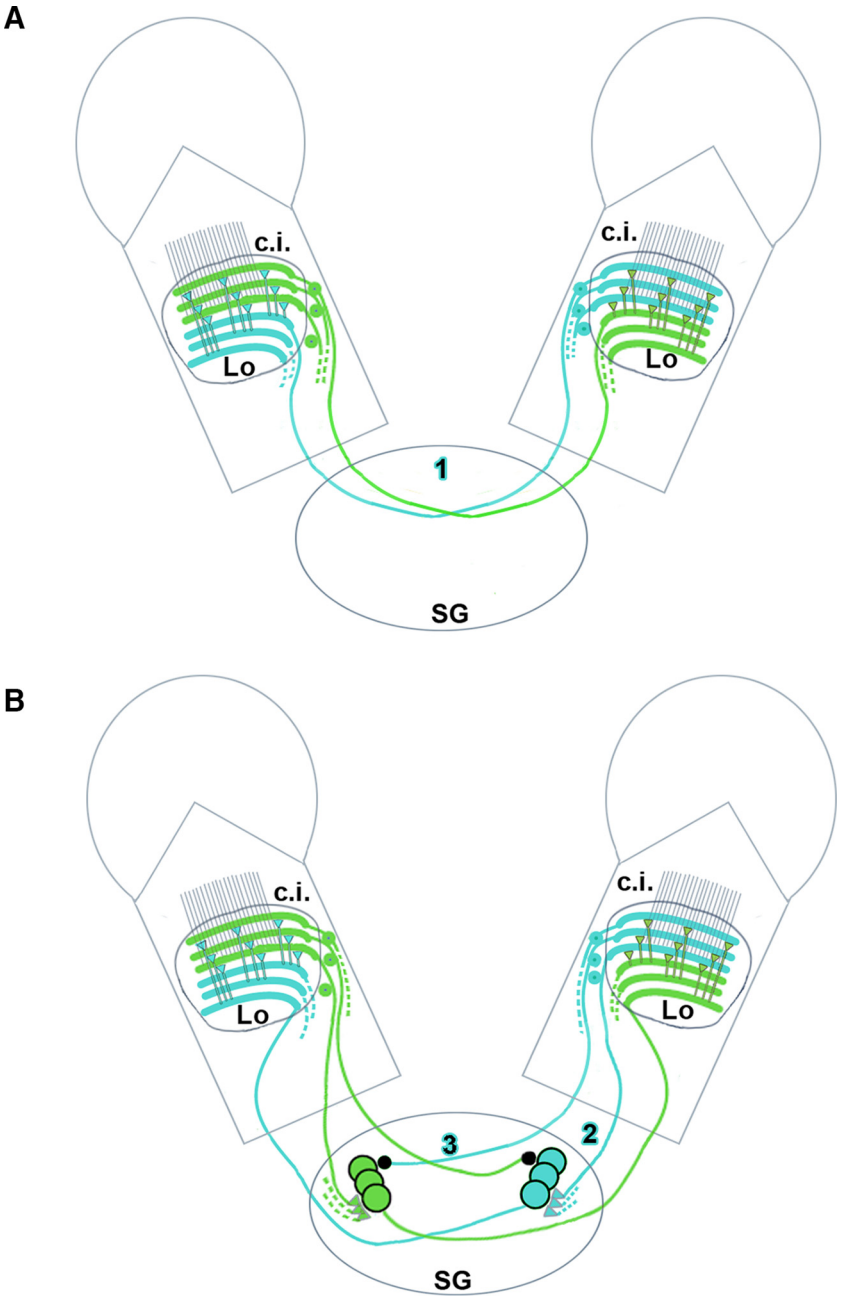

Figure 9. Schematic model of bilateral connections between LG neurons of the opposite sides according to interpretations of results from the current study. ***A***, ***B***, The scheme has been divided to facilitate understanding. Lobula giant neurons receive motion information from the ipsilateral eye through columnar inputs (c.i.), and from the contralateral eye via contralateral projecting neurons. Light blue elements represent centripetal (efferent) pathways from the right lobula neuropil that after traversing the midbrain, provide inputs to the left lobula neuropil (mirror elements are represented in green). The representations in ***A*** and ***B*** include, respectively, a direct pathway with elements projecting straight away to the opposite site (1), and less direct pathways with at least one synaptic relay in the supraesophageal ganglion (2). These pathways, here represented by sets of three elements, may include multiple neuronal units, as suggested by the high proportion of LG neurons that exhibited binocular response (Fig. 5), by the variety of responses (Fig. 4), and by the number of crossing stained fibers that can be seen in Figure 7, *A* and *B*. Triangles represent excitatory synapses and black circles inhibitory synapses. The existence of crossed inhibitory interactions (3) is warranted to explain the results of categories 2-1, 1-2, and 2-2 in Figures 4 and 5. Discontinuous lines stand for additional connecting elements similar to the ones depicted in the scheme. Multiple excitatory terminals from different units that impinge onto single units indicate that each LG would be feed by numerous units from the contralateral side. Lo, Lobula; SG, supraesophageal ganglion.

Do all types of LGs perform alike?

The four classes of LGs that had been identified vary in morphology, number of elements composing each class, receptive field size, computational features, and multisensory integration properties (Medan et al., 2007, 2015; Oliva and Tomsic, 2014, 2016; for review, see Tomsic, 2016). But they also exhibit substantial commonalities, as a strong preference for single-object motion versus panoramic optic flow, and fast habituation to repeated stimulation (Medan et al., 2007; Tomsic et al., 2003; Sztarker and Tomsic, 2011; Berón de Astrada et al., 2013; for review, see Tomsic, 2016). Based on the response preferences and other physiological criteria (Medan et al., 2007; Tomsic et al., 2017), 19 of the 42 neurons analyzed in Figure 5 could be confidently identified as follows: MLG2: 8; BLG1: 7; BLG2: 4. Within these neurons, we looked at the possibility that the different LG classes might be associated to some of the categories of binocular interaction described in this paper (Figs. 4, 5*B*). We were unable to find any reliable association. Further studies are necessary to address this issue.

What crabs can get from binocular processing?

In a previous study we have described that most LG neurons responded to object motion presented separately to each eye (Sztarker and Tomsic, 2004). However, the neurons were not assessed in the binocular condition, which prevented analyzing the monocular contributions to the binocular response, as we did here. In addition, that study was done with an object moved overhead, which corresponds to the less-sensitive visual area of the crab. In fact, crabs living in mudflat environments, like *Neohelice*, possess a rim of maximal optical resolution around the eye's equator (Berón de Astrada et al., 2012), which coincides with the center of the vertical receptive field of some LG neurons (Medan et al., 2015). These optical and neural specializations appears to be adaptations dedicated to perceiving the movements of neighboring crabs, which in a mudflat world most often occur few degrees above and below the horizon (Zeil and Hemmi, 2006; Tomsic et al., 2017). Noteworthy, mudflat crabs and *Neohelice* in particular live in high-density populations (Luppi et al., 2013), where social interactions represent the most common source of object motion that they experience. Behavioral interactions include courtship, burrow defense, running away from or chasing after other individuals (Hemmi and Zeil, 2003; Sal Moyano et al., 2014; Tomsic et al., 2017). Ongoing video analyses on the prey capture behavior of *Neohelice* indicate that at the last stage of its pursuing run, the crab jumps over the target with the claws widely opened to clench it, an ability that seems to entail a precise estimation of the target distance. Our investigation here was aimed at analyzing neuronal responses in the frontolateral visual field, the region that the animal ultimately uses to confront with rivals, capture prey, and handle food items with its claws. A proper organization of these behaviors may require or would be greatly benefited by the animal's ability to compute binocular information. Our current results show that such computations extensively occur at an early stage of the visual pathway.

References

Barnes WJP, Nalbach HO (1993) Eye movements in freely moving crabs: their sensory basis and possible role in flow-field analysis. Comp Biochem Physiol 104:675–693. CrossRef

Bengochea M, Berón de Astrada M, Tomsic D, Sztarker J (2018) A crustacean lobula plate: morphology, connections, and retinotopic organization. J Comp Neurol 526:109–119. CrossRef Medline

Berón de Astrada M, Tomsic D (2002) Physiology and morphology of visual movement detector neurons in a crab (*Decapoda*: *Brachyura*). J Comp Physiol A Neuroethol Sens Neural Behav Physiol 188:539–551. CrossRef Medline

Berón de Astrada M, Medan V, Tomsic D (2011) How visual space maps in the optic neuropils of a crab. J Comp Neurol 519:1631–1639. CrossRef Medline

Berón de Astrada M, Bengochea M, Medan V, Tomsic D (2012) Regionalization in the eye of the grapsid crab *Neohelice granulata (=Chasmagnathus granulatus)*: variation of resolution and facet diameters. J Comp Physiol A Neuroethol Sens Neural Behav Physiol 198:173–180. CrossRef Medline

Berón de Astrada M, Bengochea M, Sztarker J, Delorenzi A, Tomsic D (2013) Behaviorally related neural plasticity in the arthropod optic lobes. Curr Biol 23:1389–1398. CrossRef Medline

Collet TS (1987) Binocular depth vision in arthropods. Trends Neurosci 10:1–2. CrossRef

DeVoe RD, Kaiser W, Ohm J, Stone LS (1982) Horizontal movement detectors of honeybees: directionally-selective visual neurons in the lobula and brain. J Comp Physiol A Neuroethol Sens Neural Behav Physiol 147:155–170. CrossRef

Duistermars BJ, Care RA, Frye MA (2012) Binocular interactions underlying the classic optomotor responses of flying flies. Front Behav Neurosci 6:6. CrossRef Medline

Dunbier JR, Wiederman SD, Shoemaker PA, O'Carroll DC (2012) Facilitation of dragonfly target-detecting neurons by slow moving features on continuous paths. Front Neural Circuits 6:79. CrossRef Medline

Hemmi JM, Zeil J (2003) Robust judgement of inter-object distance by an arthropod. Nature 421:160–163. CrossRef Medline

Hennig P, Kern R, Egelhaaf M (2011) Binocular integration of visual information: a model study on naturalistic optic flow processing. Front Neural Circuits 5:4. CrossRef Medline

Horridge GA, Sandeman DC (1964) Nervous control of optokinetic responses in the crab, *Carcinus.* Proc R Soc Lond B Biol Sci 161:216–246. CrossRef Medline

Hubel DH, Wiesel DTN (1962) Receptive fields, binocular interaction and functional architecture in the cat's visual cortex. J Physiol 160:106–154. CrossRef Medline

Krapp HG, Hengstenberg R, Egelhaaf M (2001) Binocular contributions to optic flow processing in the fly visual system. J Neurophysiol 85:724–734. CrossRef Medline

Land M, Layne J (1995) The visual control of behavior in fiddler crabs: II. Tracking control systems in courtship and defense. J Comp Physiol A Neuroethol Sens Neural Behav Physiol 177:91–103. CrossRef

Livingstone MS, Conway BR (2003) Substructure of direction-selective receptive fields in macaque V1. J Neurophysiol 89:2743–2759. CrossRef Medline

Luppi T, Bas C, Méndez Casariego A, Albano M, Lancia J, Kittlein M, Rosenthal A, Farías N, Spivak E, Iribarne O (2013) The influence of habitat, season and tidal regime in the activity of the intertidal crab *Neohelice (=Chasmagnathus) granulata).* Helgol Mar Res 67:1–15. CrossRef

Medan V, Oliva D, Tomsic D (2007) Characterization of lobula giant neurons responsive to visual stimuli that elicit escape behaviors in the crab *Chasmagnathus.* J Neurophysiol 98:2414–2428. CrossRef Medline

Medan V, Berón De Astrada M, Scarano F, Tomsic D (2015) A network of visual motion-sensitive neurons for computing object position in an arthropod. J Neurosci 35:6654–6666. CrossRef Medline

Nalbach HO, Thier P, Varjú D (1993) Binocular interaction in the optokinetic system of the crab *Carcinus maenas* (L.): optokinetic gain modified by bilateral image flow. Vis Neurosci 10:873–885. CrossRef Medline

Nityananda V, Tarawneh G, Rosner R, Nicolas J, Crichton S, Read J (2016) Insect stereopsis demonstrated using a 3D insect cinema. Sci Rep 6:18718. CrossRef Medline

Oliva D, Tomsic D (2014) Computation of object approach by a system of visual motion-sensitive neurons in the crab *Neohelice.* J Neurophysiol 112:1477–1490. CrossRef Medline

Oliva D, Tomsic D (2016) Object approach computation by a giant neuron and its relation with the speed of escape in the crab *Neohelice.* J Exp Biol 219:3339–3352. CrossRef Medline

Ramdya P, Engert F (2008) Emergence of binocular functional properties in a monocular neural circuit. Nat Neurosci 11:1083–1090. CrossRef Medline

Rosner R, Homberg U (2013) Widespread sensitivity to looming stimuli and small moving objects in the central complex of an insect brain. J Neurosci 33:8122–8133. CrossRef Medline

Sal Moyano MP, Gavio MA, Mclay CL, Luppi T (2014) Variation in the postcopulatory guarding behavior of *Neohelice granulata* (Brachyura, Grapsoidea, Varunidae) in two different habitats. Mar Ecol 36:1185–1194. CrossRef

Scarano F, Tomsic D (2014) Escape response of the crab *Neohelice* to computer generated looming and translational visual danger stimuli. J Physiol Paris 108:141–147. CrossRef Medline

Smolka J, Hemmi JM (2009) Topography of vision and behaviour. J Exp Biol 212:3522–3532. CrossRef Medline

Sombke A, Harzsch S (2015) Immunolocalization of histamine in the optic neuropils of *Scutigera coleoptrata* (Myriapoda: Chilopoda) reveals the basal organization of visual systems in mandibulata. Neurosci Lett 594: 111–116. CrossRef Medline

Strausfeld NJ (2009) Brain organization and the origin of insects: an assessment. Proc Biol Sci 276:1929–1937. CrossRef Medline

Strausfeld NJ, Nässel DR (1981) Neuroarchitecture of brain regions that subserve the compound eyes of Crustacea and insect. In: Handbook of sensory physiology: vision in invertebrates, Vol. VII/6B (Autrum, ed), pp 1–32. Berlin; Heidelberg; New York: Springer.

Suver MP, Huda A, Iwasaki N, Safarik S, Dickinson MH (2016) An array of descending visual interneurons encoding self-motion in *Drosophila*. J Neurosci 36:11768–11780. CrossRef Medline

Suzuki Y, Morimoto T, Miyakawa H, Aonishi T (2014) Cooperative integration and representation underlying bilateral network of fly motion-sensitive neurons. PLoS One 9:e85790. CrossRef Medline

Sztarker J, Tomsic D (2004) Binocular visual integration in the crustacean nervous system. J Comp Physiol A Neuroethol Sens Neural Behav Physiol 190:951–962. CrossRef Medline

Sztarker J, Tomsic D (2011) Brain modularity in arthropods: individual neurons that support "what" but not "where" memories. J Neurosci 31: 8175–8180. CrossRef Medline

Tomsic D (2016) Visual motion processing subserving behavior in crabs. Curr Opin Neurobiol 41:113–121. CrossRef Medline

Tomsic D, Berón de Astrada M, Sztarker J (2003) Identification of individual neurons reflecting short- and long-term visual memory in an arthropod. J Neurosci 23:8539–8546. CrossRef Medline

Tomsic D, Sztarker J, Berón de Astrada M, Oliva D, Lanza E (2017) The predator and prey behaviors of crabs: from ecology to neural adaptations. J Exp Biol 220:2318–2327. CrossRef Medline

Wertz A, Borst A, Haag J (2008) Nonlinear integration of binocular optic flow by DNOVS2, a descending neuron of the fly. J Neurosci 28:3131–3140. CrossRef Medline

Wiersma CA, Bush BM, Waterman TH (1964) Efferent visual responses of contralateral origin in the optic nerve of the crab podophthalmus. J Cell Comp Physiol 64:309–326. CrossRef Medline

Wood HL, Glantz RM (1980a) Distributed processing by visual interneurons of crayfish brain. I. response characteristics and synaptic interactions. J Neurophysiol 43:729–740. CrossRef Medline

Wood HL, Glantz RM (1980b) Distributed processing by visual interneurons of crayfish brain: II. Network organization and stimulus modulation of synaptic efficacy. J Neurophysiol 43:741–753. CrossRef Medline

Zeil J, Hemmi JM (2006) The visual ecology of fiddler crabs. J Comp Physiol A 192:1–25. CrossRef